A Study of a Firefly Meta-Heuristics for Multithreshold Image Segmentation

H. Erdmann, G. Wachs-Lopes, C. Gallão, M. P. Ribeiro and P. S. Rodrigues

Abstract Thresholding-based image segmentation algorithms are usually developed for a specific set of images because the objective of these algorithms is strongly related to their applications. The binarization of the image is generally preferred over multi-segmentation, mainly because it's simple and easy to implement. However, in this paper we demonstrate that a scene separation with three threshold levels can be more effective and closer to a manually performed segmentation. Also, we show that similar results can be achieved through a firefly-based meta-heuristic. Finally, we suggest a similarity measure that can be used for the comparison between the distances of the automatic and manual segmentation.

1 Introduction

Image segmentation is a task with applications in several areas related to digital image processing. It can be done by estimating the number of thresholds used to partition an image into regions of interest. The most simple thresholding technique is to divide the image in two regions, binarizing the search space.

Among the known techniques to define a threshold that splits an image in two clusters, there are those based on the probabilistic-distribution entropy for the color intensities. In [1], T. Pun wrote the first algorithm for image binarization based on the traditional Shannon entropy, assuming that the optimal threshold is the one that

H. Erdmann (✉) · G. W. -Lopes · C. Gallão · P. S. Rodrigues
Inaciana Educational Foundation, Sao Bernardo do Campo, Sao Paulo, Brazil
e-mail: horste@fei.edu.br

G. W. -Lopes
e-mail: gwachs@fei.edu.br

C. Gallão
e-mail: celsogallao@hotmail.com

M. P. Ribeiro
Federal University of Viçosa, Viçosa, Minas Gerais, Brazil
e-mail: monael@gmail.com

P. S. Rodrigues
e-mail: psergio@fei.edu.br

J. M. R. S. Tavares, R. Natal Jorge (eds.), *Developments in Medical Image Processing and Computational Vision,* Lecture Notes in Computational Vision and Biomechanics 19,
DOI 10.1007/978-3-319-13407-9_17

maximizes the additivity property for its entropy. Such property states that the total entropy for a whole physical system (represented by its probability distribution) can be calculated from the sum of entropies of its constituent subsystems (represented by their individual probability distributions).

Kapur et al. [2] maximized the upper threshold of the maximum entropy to obtain the optimal threshold, and Abutaleb [3] improved the method using bidimensional entropies. Furthermore, Li and Lee [4] and Pal [5] used the direct Kullback-Leibler divergence to define the optimal threshold. And some years before, Sahoo et al. [6] used the *Reiny*-entropy seeking the same objective. More details about these approaches can be found in [7], which presents a review of entropy-based methods for image segmentation.

Considering the restrictions of Shannon entropy, Albuquerque et al. [8] proposed an image segmentation method based on Tsallis non-extensive entropy [9], a new kind of entropy that is considered as a generalization of Shannon entropy through the inclusion of a real parameter q, called "non-extensive parameter". The work of Albuquerque [8] showed promising results and a vast literature demonstrating the performance of this method against the Optimal Threshold Problem. Although it is a new contribution to the field, this paper will not address the Tsallis entropy.

A logical extension of binarization is called multi-thresholding [10, 11], which consider multiple thresholds on the search space, leading to a larger number of regions in the process of segmentation.

However, since the optimal threshold calculation is a direct function of the thresholds quantity, the time required to search for the best combination between the thresholds tends to grow exponentially. Furthermore, the optimum quantity of thresholds is still a topic for discussion. Thus, the literature has proposed the use of meta-heuristics that may be efficient for the calculation of thresholds, one of them being the Firefly.

Recently, M. Horng [11] proposed an approach based on Minimum Cross-Entropy thresholding (MCET) for multilevel thresholding with the same objective function criterion as proposed by P. Yin [10]. The main conclusion of the work was that the Cross-Entropy based method, a linear time algorithm, obtained thresholds values very close to those found by equivalent exhaustive search (brute-force) algorithms. However, the results were inconclusive since their methodology to evaluate the experiment was subjective.

This article proposes an analysis of the Firefly meta-heuristics for multi-threshold-based image segmentation. We also present the use of a Golden Standard Image Base that allows us to compare the segmentation results of different algorithms in an objective manner.

2 The Proposed Methodology

The strategy used in this study is the comparison of the obtained results with exhaustive methods results, both manual and automatic. Although these methods have polynomial complexity in $O(n^{d+1})$ order, where d and n are the number of thresholds and histogram bins respectively. It is computationally expensive to calculate the results for $d \geq 3$.

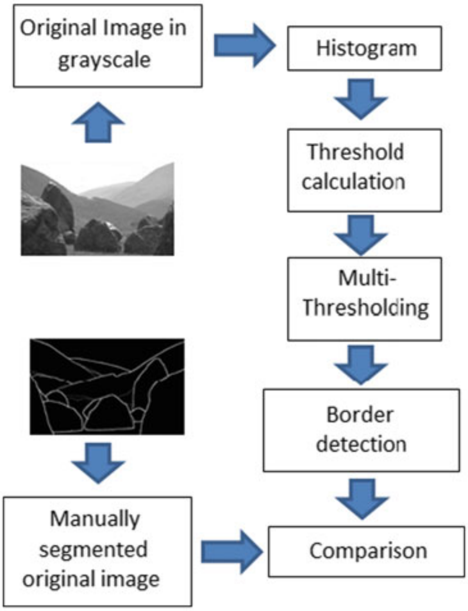

Fig. 1 Proposed comparison methodology scheme. The first row shows an example of original image and its manual segmentation taken as a basis of comparison

One important issue is to define the number of thresholds required to obtain a segmentation result as close as possible to that obtained manually. The answer seems subjective and dependent on cognitive factors that are outside the scope of this paper. Thus, the database used for comparison of the results consists of several images that were manually segmented during psychophysical experiments that were defined and performed in [12]. Moreover, the results will be compared in two directions. First, we compare the results of the exhaustive segmentation with the respective manual one. Then, we compare the results of the manual segmentation with the ones obtained with the Firefly meta-heuristics, allowing us to draw a comparison between both methods used.

Although answering cognitive questions is not the purpose of this paper, the exhaustive search of the entire result space, allows us to observe the minimum amount of thresholds required to obtain the closest result to the manual segmentation. This lower limit can be used for any segmentation algorithms besides those cited in this paper. The method used to compute the threshold-based multi segmentation with the Firefly meta-heuristics is shown in Fig. 1.

3 Firefly Meta-Heuristics

The Firefly (FF) algorithm was proposed by Xin-She Yang [13] and is a meta-heuristics inspired on the fireflies behavior, which are attracted among themselves according to their natural luminescence.

After their interactions, convergence is achieved through the creation of fireflies clusters, on which the brighter attract the less bright ones under certain restrictions, such as: (i) all fireflies are unisex so that one firefly will be attracted to any other fireflies regardless of their sex; (ii) attractiveness is proportional to their brightness, thus for any two flashing fireflies, the less bright one will move towards the brighter one, remembering that the glow dimishes as the distance between them increases; (iii) if, for any given firefly, there isn't any other brighter firefly, than it moves randomly.

The general idea is modeling a non-linear optimization problem by associating each problem's variable to a firefly and make the objective evaluation depending on these variables, which are associated to the fireflies brighten. Then, iteratively, the variables are updated (their brightens) under preestablished rules until the convergence to a global minimum. Generically, it is accomplished at each generation, according to the following main steps:

- bright evaluation;
- compute all distances between each par of fireflies;
- move all fireflies one toward all others, according to their brightens;
- keep the best solution (the brighter firefly);
- generate randomly new solutions;

The kernel of the algorithm is its Z-function evaluation, which depends on the current problem. Specifically for multi-level thresholding problem, as proposed in [13, 11] and [14], each firefly is considered a d-dimensional variable, where each dimension is a distinct threshold, partitioning the histogram space. In the specific case of the reference [14], the goal is to minimize an objective function under the non-extensive Tsallis entropy criterium of intensity histogram associated to each image to be segmented. The Algorithm 1, reproduced from [14], shows this idea in a more formal perspective, where the set of n initial firefly solutions is given in line 4. Each firefly f_i is a d-dimensional vector and x_k^i is the k-th threshold of the i-th firefly solution f_i.

In this implementation, for any firefly f_i, the strength of attractiveness for other brighter firefly f_j can be given by the update rule from lines 12 to 23. This equation states that at each iteration t, the solution f_i depends mainly on the f_j solution and the bright differences $r_{i,j}$ of all fireflies j, and the new random solution μ_t, which is drawn from a Gaussian or other distribution. The bright of a firefly i is only updated when i is less brighter than any other firefly j. Such update is proportional to the attractiveness factor β, the absorption coefficient γ and the step motion α.

The objective Z-function very much influences the final result and is application dependent. In this paper, we consider multi-level image thresholding problems in the step two of the proposed methodology and we investigate how the traditional Shannon entropy [1] and its generalization Tsallis entropy [8] influences in the final results of the proposed CAD system.

The algorithm is designed to model a non-linear optimizer associating the thresholds to fireflies. The kernel depends on these variables, which are associated with the fireflies glow and can be modified according to be more appropriate to the data

Algorithm 1 Firefly Algorithm to MLTP (adapted from [11])

Input: n : number of fireflies;
d: dimension;
γ: absorbing coefficient;
α: motion;
β: attracting factor;
MG: maximum number of generations;
Output: acceptable threshold set $f_i^* = \{x_1^i, x_2^i, \ldots, x_d^i\}$
Define initial values: $t = 0$, $\alpha_0 = 1.0$
Randomly define the initial population $\{f_1, f_2, \ldots, f_n\}$ where $f_i = \{x_1^i, x_2^i, \ldots, x_d^i\}$ is the i-th d-dimensional solution of the firefly
while $t \leq MG$ **do**
  for $i = 1 \to n$ **do**
    for $j = 1 \to n$ **do**
      Calculate the $r_{i,j}$ distance between the glows $Z(f_i)$ and $Z(f_j)$
    end for
  end for
  for $i = 1 \to n$ **do**
    Glow evaluation $Z(f_i)$ using Tsallis entropy
    for $j = 1 \to n$ **do**
      if $Z(f_i)$ is less bright than $Z(f_j)$ **then**
        Move the f_i firefly towards the f_j firefly, according to the following update rule:
        Randomly generate a new solution $\mu_t = \{x_1, x_2, \ldots, x_d\}$
        $\alpha_t = \alpha\alpha_t$
        $\beta_0 = \beta \exp(-\gamma r_{i,j}^2)$
        for $k = 1 \to d$ **do**
          $x_k^i = (1 - \beta_0)x_k^i + \beta_0 x_k^j + \alpha_t \mu_t$
        end for
      end if
    end for
  end for
  Sort the fireflies according to their glow $Z(.)$
  Define the brightest firefly f_i^* as the current result
  $t = t + 1$
end while

that is being manipulated. Then, the fireflies luminescences are updated iteratively under pre-established rules until the algorithm convergence to a global minimum.

The papers of Lukasik and Zak [15] and Yang [13] suggest that the FF overcome other meta-heuristics, such as the Ant Farm [16], Tabu search [17], PSO [18] and Genetic Algorithms [19]. Thus, the FF was presented as a computing-time efficient method to the Multilevel Thresholding Problem (MLTP). Recently, the work of [20] showed a computational time comparison of the FF against the other method, demonstrating that the FF is more efficient when the evaluation function is modeled with the maximum inter-cluster variance. Other works, such as [11] and [10] also showed similar results when applied to the MLTP.

Specifically for the MLTP modeling, each firefly is a d-dimensional vector, where each dimension is a single threshold that partitions the histogram space. In the specific work of M. H. Horng and R. J. Liou [11], the goal was to minimize the objective function using the Cross-Entropy of the intensities histogram associated with each segmented image criteria.

The Algorithm 1 describes the FF, where a solution set of n initial fireflies is given on line 3. Each firefly f_i is a d-dimensional vector and x_k^i is the k-th threshold of i-th solution. More details about the FF can be found in [11] and [13].

4 The Entropy Criteria for Evaluation Functions

In this paper we show the results obtained using a novel approach for the firefly algorithm. Our contribution is the use of Tsallis non-extensive entropy as a kernel evaluation function for the firefly algorithm. This type of entropy is described in the following sections.

4.1 *The Shannon Entropy*

The very celebrated Shannon entropy has been achieved several applications since C. Shannon proposed it for information theory [21]. Considering a probability distribution $P(H) = \{h(1), h(2), \ldots, h(n)\}$., the Shannon entropy, denoted by $S(H)$, is defined as:

$$S(H) = -\sum_{i=1}^{L} h_i \log(h_i) \tag{1}$$

As stated before, T. Pun [1] applied this concept for 1LTP through the following idea. Let two probability distributions from $P(H)$, one for the foreground, $P(H_1)$, and another for the background, $P(H_2)$, given by:

$$P(H_1) : \frac{h_1}{p_A}, \frac{h_2}{p_A}, \ldots, \frac{h_t}{p_A} \tag{2}$$

$$P(H_2) : \frac{h_{t+1}}{p_B}, \frac{h_{t+2}}{p_B}, \ldots, \frac{h_L}{p_B} \tag{3}$$

where $p_A = \sum_{i=1}^{t} p_i$ and $p_B = \sum_{i=t+1}^{L} p_i$.

If we assume that H_1 and H_2 are independent random variables, then the entropy of the composed distribution[1] verify the so called additivity rule:

$$S(H_1 * H_2) = S(H_1) + S(H_2). \tag{4}$$

[1] we define the composed distribution, also called direct product of $P = (p_1, \ldots, p_n)$ and $Q = (q_1, \ldots, q_m)$, as $P * Q = \{p_i q_j\}_{i,j}$, with $1 \leq i \leq n$ and $1 \leq j \leq m$

In the case of 1LTP, the optimal threshold t^* is that one which maximizes the Eq. (4), which can be computed in $O(L^2)$ time.

As before, by assuming independent distributions and under the same normalization restrictions, it is easy to extend the Eq. (4) for the case of $d > 1$ partitions, to obtain the following generalization of the additive rule:

$$S(H_1 * H_2 * \cdots * H_{d+1}) = S(H_1) + S(H_2) + \cdots + S(H_{d+1}) \tag{5}$$

which, as in the case of cross-entropy, requires $O(L^{d+1})$ in order to achieve the set of d optimal thresholds that maximizes the entropy in Expression (5).

4.2 The Non-Extensive Tsallis Entropy

As mentioned before, the Tsallis entropy is a generalization of the Shannon one (see [22] and references therein). The non-extensive Tsallis entropy of the distribution $P(H)$, denoted by $S_q(H)$, is given by:

$$S_q(H) = \frac{1 - \sum_{i=1}^{L} h_i^q}{1 - q} \tag{6}$$

The main feature observed in Eq. (6) is the introduction of a real parameter q, called non-extensive parameter. In [9] it is shown that, in the limit $q \to 1$, Eq. (6) meets the Eq. (1).

For Tsallis entropy we can find an analogous of the additivity property (Expression (4)), called pseudo-additivity due to the appearance of an extra term. For 1LTP ($d = 1$), given two independent probability distributions $P(H_1)$ and $P(H_2)$ from $P(H)$, the pseudo-additivity formalism of Tsallis entropy is given by the following expression:

$$S_q(H_1 * H_2) = S_q(H_1) + S_q(H_2) + (1 - q)S_q(H_1)S_q(H_2) \tag{7}$$

where $S_q(H_1)$ and $S_q(H_2)$ are calculated by applying Eq. (6) for the probability distributions $P(H_1)$ and $P(H_2)$.

For this 1LTP, the optimal threshold t^* is the one that maximizes the pseudo-additivity property (7), and is computed in $O(L^2)$. As in the case of Shannon entropy, we can easily derive a generalized version of Eq. (7) given by:

$$\begin{aligned} S_q(H_1 * \cdot * H_{d+1}) = S_q(H_1) + \cdots + S_q(H_{d+1}) + \\ (1 - q)S_q(H_1)S_q(H_2) \ldots S_q(H_{d+1}) \end{aligned} \tag{8}$$

which is useful for MLTP. However, for the same reasons of cross-entropy and Shannon entropy, the computational time for solving the corresponding MLTP (without a recursive technique) is $O(L^{d+1})$.

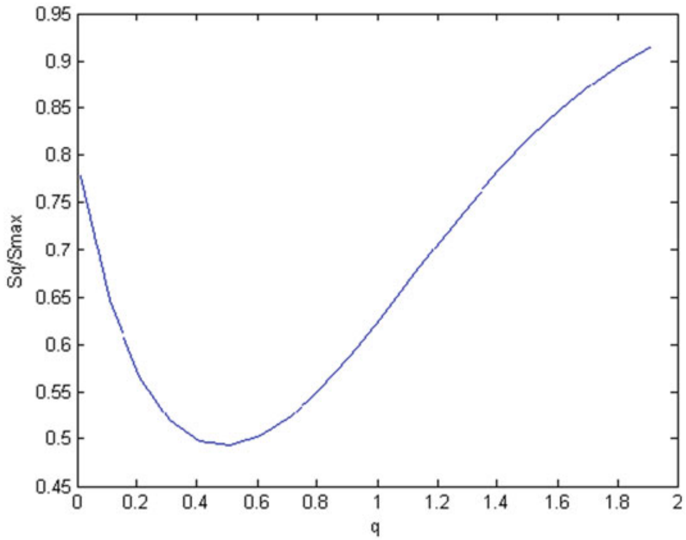

Fig. 2 Adapted from [24]. Automatic q value calculation. In this figure it is possible to see that the optimum value of q is 0.5

As Shannon Entropy (SE), Tsallis Entropy (TE) also tries to balance mutual information between partitions of a distribution, since it depends on the individual probabilities instead of their positions. Note that the parameter q powers the probability values, given a fine tuning in the pseudo-additivity maximization.

4.3 Automatic q Calculation

The main downside of the Tsallis entropy used by researchers such as Albuquerque et al. [8], and Rodrigues et al. [23], is the definition of the q parameter that usually is done manually. Thus, Rodrigues and Giraldi proposed a novel method for the automatic calculation of q value [24]. Since the maximal entropy of a probabilistic distribution X occur when all states of X, $(x_1, x_2, \ldots, x_n)$ have the same probability. So the maximum entropy of the X distribution, S_{MAX}, is given by Eq. (9).

$$S_{MAX} = \frac{1}{q-1}\left[1 - n(p^q(x))\right] \tag{9}$$

where: q is the entropic parameter and n is the amount of elements of the X distribution.

From the point of view of information theory , the lesser the relation between the entropy S_q produced by a q value and the maximal entropy S_{MAX} of a system, the greater is the information contained in that system. This is a well-known concept of the information theory and gives us the idea that an optimum q value can be calculated by minimizing the S_q/S_{MAX} function [24].

Thus for each distribution, we calculate the values of the relations between the S_q entropy and the maximal entropy S_{MAX} for each value of q varying in the range of $[0.01, 0.02, \ldots, 2.0]$ in order to find the q value that minimizes the relation. In Fig. 4, one can observe the behavior of the relation between S_q and S_{MAX} throughout the q variation.

5 The Image Database

In this work, we made use of 300 images from the Berkeley University database [12]. Such images are composed of various natural scenes, wherein each was manually segmented. The task to segment an image into different cognitive regions is still an open problem. It is possible to highlight two main reasons for it to be considered a difficult task: (i) a good segmentation depends on the context of the scene, as well as from the point of view of the person who is analyzing it; and (ii) it is rare to find a database for formal comparison of the results. Generally, researchers present their results comparing just a few images, pointing out what they believe is correct. In these cases, probably the same technique will work only with other images that belong to the same class. Still, the question that remains unresolved is: "What is a correct segmentation?".

In the absence of an answer to the question, a reference is necessary that allows the comparison of several techniques under the same database or parametrization. Regarding this, the image database used here can be considered as an attempt to establish such reference.

The Fig. 3 shows many examples of the pictures that belong to the database and the overlapping of 5 edge-maps derived from the manual segmentation, which denotes the high level of consistency between segmentations done by different persons. Additional details about this image database can be read on [12].

When overlapping the five edge-maps of the same image as in Fig. 3, some edges do not match, thus the final intensity of each edge of the overlapped image is going to be higher if it overlaps more edges and less intense otherwise. In this article, we made use of 300 images as comparison base (gold standard) for our experiments.

Furthermore, the divergence of information in the absolute value between the automatically-obtained segmentations and the golden standard (manually-obtained segmentations) were also not considered as a segmentation-quality measure. So, the image database is used as a tool for comparison between the results of the two evaluated methods.

6 Similarity Measure

We defined a function to measure the similarity between the manual and the automatic segmentation. However, this is a difficult task and the problem is still unsolved. Sezgin and Sankur [25] proposed 5 quantitative criteria for measuring the luminance

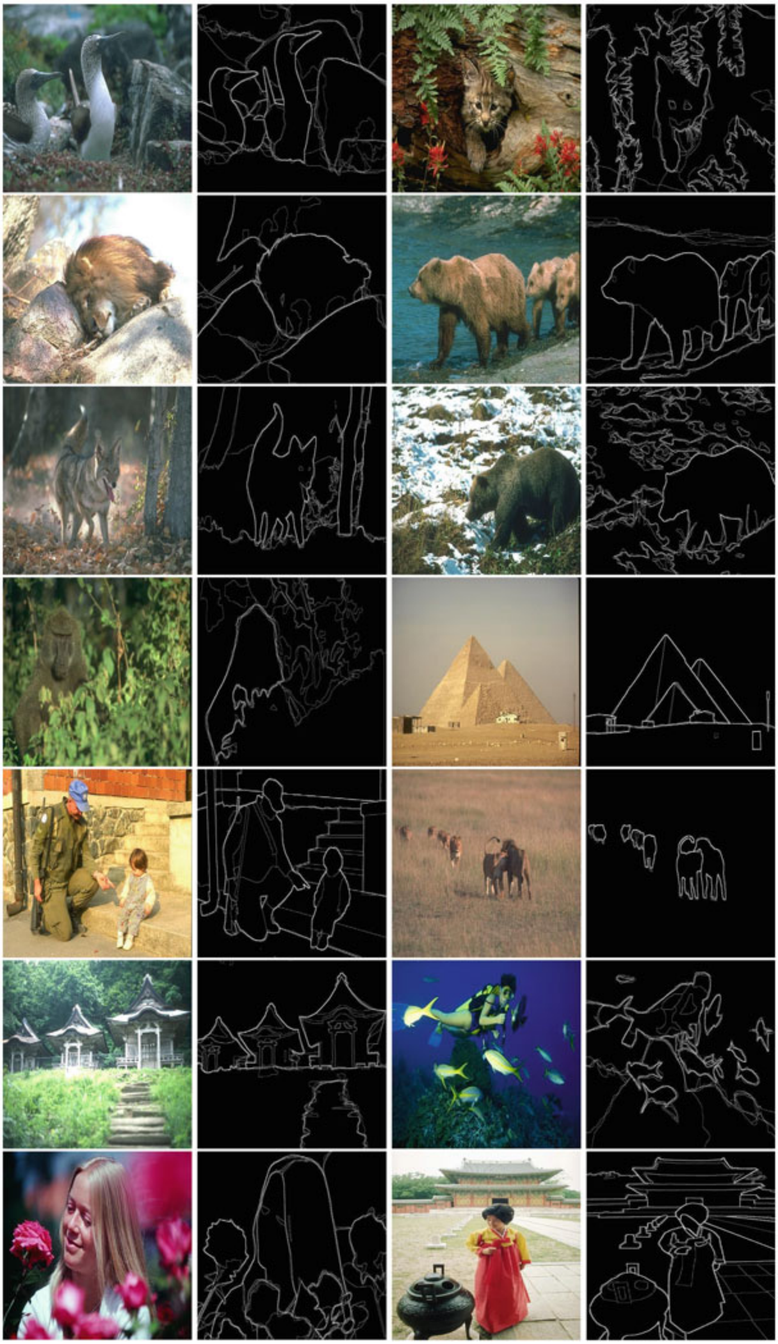

Fig. 3 Sample images from the Berkley University database [12] composed of 300 manually segmented images used on the experiments as ground truth

region and shaped 20 classical methods to measure the similarity between them. But the criterion they proposed was not based on a golden standard defined set of images, thus the method of comparison proposed in [25] can be used only as an intrinsic quality evaluation of the segmented areas: i.e, one output image segmented into uniformly molded regions cannot be considered as close as expected to the manual segmentation.

On the other side, golden standard based measuring techniques are also difficult to propose when the system needs to detect several regions of the image at the same time, a common task in computer vision. Besides that, to compare corresponding edges brings difficulty to detect entire regions, as well as their location in space. Also, in the area of computer vision, is an important demand to be able to deduct regions that are interrelated.

Although it is possible to design an algorithm which tolerates localization errors, it is likely that detecting only the matching pixels and assuming all others are flaws or false positive and may provide a poor performance.

One can speculate from Fig. 3 that the comparison between the edge-maps derived from the automatic and manual segmentations must tolerate localization errors as long as there are also divergences on the edges of the golden standard. Thus, the consideration of some differences can be useful in the final result as shown in [12].

On the other hand, from 2D edge-maps, such as the one we used, one can obtain two types of information: geometrical dispersion and intensity dispersion. The geometric dispersion measures the size and the location of the edges; the intensity dispersion measures how common is that edge among all manual segmentations that were overlapped. Thus, the geometric dispersion between two edge-maps has its information measured in a quantitative manner, in the x and y dimensions, while the luminance dispersion can be represented by the z dimension.

The divergence of information between the two edge-maps of an $M \times N$ image in the x dimension is calculated by the Euclidean distance between the two maps, where the H_x as vertical projection at the edge map for automatic segmentation and the M_x is the corresponding vertical projection for the manual one.

So, in this article, we propose a similarity function between the two edge-vertical-projection M_x and H_x of the x dimension presented in Eq. (10) to measure how different the automatically-obtained segmentation (AS_x) is from the manual one (golden standard, GS_x), in this specific direction:

$$Sim_x(GS_x|AS_x) = \sqrt{\sum_{i=1}^{M}(M_x(i) - H_x(i))^2}, \tag{10}$$

where M is the size of x distribution, M_x and H_x are the image edges projections in the x direction, manual and automatic respectively. M_x and H_x are obtained by sum of values greater than 0 in each column.

Similarly, the corresponding function to y direction is given for

$$Sim_y(GS_y|AS_y) = \sqrt{\sum_{i=1}^{N}(M_y(i) - H_y(i))^2}, \tag{11}$$

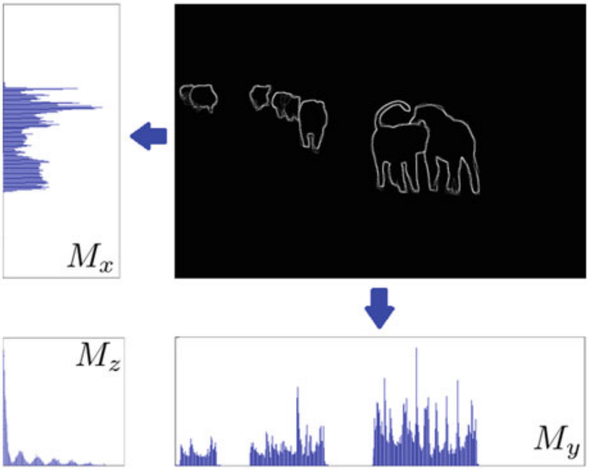

Fig. 4 Method used to obtain the vertical (M_x) and horizontal (M_y) projections of the edge map. The M_z distribution is the grayscale histogram

where N is the size of y distribution and M_y and H_y are obtained by sum of values greater than 0 in each line. The corresponding function to z direction is given for

$$Sim_z(GS_z|AS_z) = \sqrt{\sum_{i=0}^{L} (M_z(i) - H_z(i))^2}, \tag{12}$$

where $L = [0, 1, ..., 255]$ is the total of image gray levels. AS_z and GS_z represent the grayscale histogram.

Thus, in this study, we propose the following evaluation function to measure the similarity between two edge-maps:

$$Sim(GS|AS) = Sim_x + Sim_y + Sim_z \tag{13}$$

7 Experiments and Discussion

The methodology shown in Fig. 1 describes both scenarios used in this paper: (i) the segmentation with 1, 2 and 3 thresholds found by an exhaustive search; and (ii) the segmentation with 1, 2 and 3 thresholds obtained with the use of the FF meta-heuristic.

The main reason for using the exhaustive search was to guarantee that the whole solution space is explored in order to find the thresholds that provide the closest results to the golden standard for each image.

The authors of [13] and [11] presented multi-thresholding approaches based on the FF algorithm and made a comparison with the exhaustive strategy, where the FF's kernel was chosen as being the Cross-Entropy approach. This type of comparison is limited, since it is only a relative matching between the FF result and the one obtained with the entropic method (achieved in an exhaustive manner). So there is no way of knowing if there are other better solutions (threshold levels), since the search space was not entirely explored. Another limitation of the method presented in [13] and [11] is the similarity measure used, since they used the noise difference of each segmentation as a metric.

In this article the two limitations listed above were addressed in the following manner: we explored the entire solution space, for 1, 2 and 3 thresholds, ensuring that there was no better solution from the similarity measure point of view. And we also used the manually segmented image set presented previously as the basis for comparing the results of our experiments.

7.1 Exhaustive Segmentation

As in Fig. 1, we applied a threshold (1 level) for each image. Then, for each possible threshold, the image was segmented. Then we applied a gradient-based edge detector which returns the boundaries of the regions that were found. Next, the comparison between the newly obtained edge-map and the golden standard is given by Eq. (13). If $T = \{t_1, t_2, \ldots, t_L\}$, where $L = 256$, then the optimal threshold $t_{opt} \in T$ is the one that minimizes Eq. (13). These procedure was then repeated for 2 and 3 levels, remembering that the solutions space grows exponentially, since we need $|T|^2$ and $|T|^3$ tests for segmentating with 2 and 3 levels respectively.

Despite being an exhaustive strategy, the algorithm surely returns the optimal results. This means that no other thresholding-based segmentation algorithm can outmatch this algorithm's results because it searches through all possible threshold combinations in the solution's space. Thus, the distance between the exhaustive search and the Golden Standard are the lowest possible and can be used as a lower boundary for minimizing the Eq. (13). This strategy is more appropriate than the noise minimization that was proposed in [13] and [11].

If $I = \{i_1, i_2, \ldots, i_{300}\}$ is the 300 image set, for each $i_j \in I$, we can associate an array $S_i = [s_{i1}, s_{i2}, s_{i3}]$, where s_{i1} is the value given by Eq. (13) for the binarization of i_j with the optimal t_{opt}; s_{i2} is the following value for the multi-thresholding of i_j with the optimal thresholds $\{t_{opt1}, t_{opt2}\} \in T$; and finally, s_{i3} is the corresponding array with 3 thresholds $\{t_{opt1}, t_{opt2}, t_{opt3}\} \in T$.

For better visualization of the results, we created an $M_{300\times 3}$ matrix, where each M_{ij} ($1 \le i \le 300$ and $1 \le j \le 3$) element is the value of $s_{ij} \in S_i$ associated with the i image. Each i line of M was normalized into 3 intensity values $L \in \{0, 128, 255\}$, so that $M_{ij} = 0$ if $s_{ij} = max S_i$; $M_{ij} = 255$, if $s_{ij} = min S_i$; and $M_{i,j} = 128$, if s_{ij} is the median of S_i. The Fig. 5 shows M as one single image with dimensions 300×3 resized to 300×300 for better visualization.

Thus, for cell (i, j) of M on Fig. 5, the brighter the pixel, the more the image segmented with the j-th threshold resembles the manually segmented image. The darker the pixel, greater the difference between them.

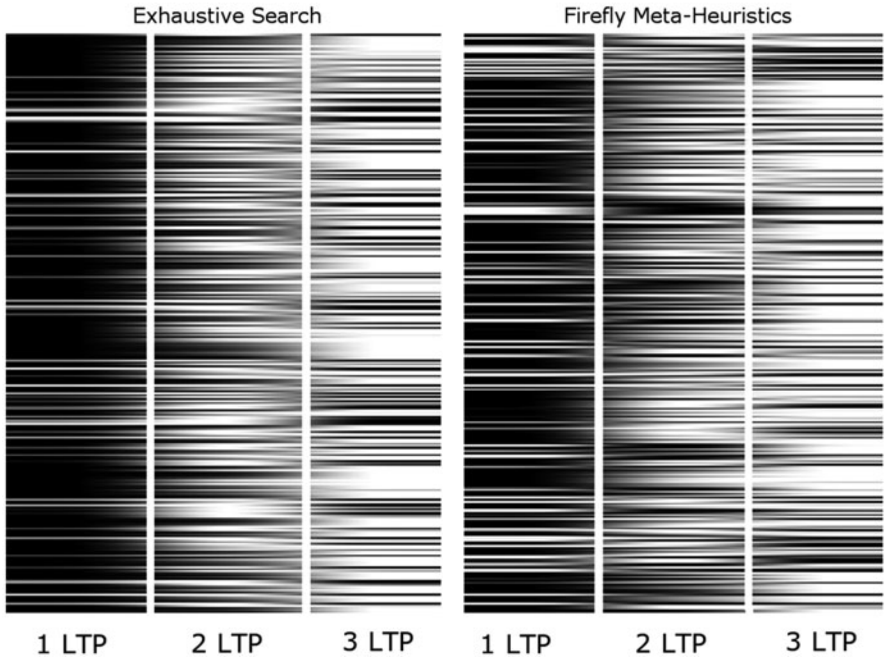

Fig. 5 Exhaustive segmentation results (*left*) and FF Meta-Heuristics segmentation results (*right*). Each row represents one of the 300 images from the database. The columns are the results of the segmentation with 1, 2 and 3 thresholds. For each row, the brighter the column, the more the image segmented with the corresponding threshold resembles the manually segmented image

7.2 Segmentation with the Firefly Meta-Heuristics

The experiments were repeated using the FF segmentation, except for the threshold calculation, that is done with the Algorithm 1. Just like the experiments with the exhaustive search method, we also created a $M_{300\times3}$ matrix with the same properties as the previous one. Comparing the Fig. 5, it is possible to notice a similarity between them, indicating that the FF results are close to the exhaustive method.

7.3 Discussion

Looking closer to the Fig. 5, one can perceive a gradient from dark to bright in both methods used, so that, for most rows (images), the columns that correspond to the segmentation with 3 thresholds are brighter (more similar) than the others. This means that, in our experiments, segmentating an image into 4 levels (3 thresholds), generally, gives us better results than with lesser threshold levels. The opposite applies to the first column, which is darker than the other 2, meaning that although

Table 1 Comparison between the exhaustive search (BF) and the FF results

Avg. Dist. with GS	Exhaustive search	Firefly algorithm	Difference (%)
FF = BF	21.41	24.15	11.33
FF $\neq$ BF	21.36	23.69	9.85
Total	21.39	23.93	10.61

Table 2 Quantitative comparison between the exhaustive search (BF) and the FF results

Threshold results	Exhaustive search	Firefly algorithm
1 Threshold	5	53
2 Thresholds	114	73
3 Thresholds	181	174
1 Threshold (when FF=BF)	1	1
2 Thresholds (when FF=BF)	36	36
3 Thresholds (when FF=BF)	116	116

it's the fastest and easiest way to segmentate an image, binarizing generally produces the worst segmentation results when compared with the results obtained with more thresholds.

In a more detailed analysis, we listed on Table 1 a general comparison between the results of the FF Meta-Heuristics and the exhaustive search (or brute-force, BF). The columns 2 and 3 represent the average distance between the golden standard (GS) and the BF and FF methods respectively. The last column represents the percent difference between the FF and BF. The first line describes the average distances when the BF and the FF thresholds are equal. The second line lists the distances when the results are not equal. And the final line summarizes all the results.

The main observation that can be made from the results listed on Table 1 is that the FF algorithm's results are very close to the exhaustive search. The average difference between them is 10.61 %. This shows that even when the FF does not find the optimum threshold, the distance between the segmentation obtained from its result is only 10.61 % different from the desired. As the threshold quantity grows, the levels combination tends to a combinatory explosion that causes the exhaustive search method to be impossible to calculate. The FF methods responds well in these cases, finding a result that is only 10.61 % different from the optimum but with linear processing time.

The Table 2 describes a quantitative comparison between the exhaustive search and the FF Meta-Heuristics. On the first line, it shows how many images where best segmented with 1 threshold with the BF and the FF methods (columns 2 and 3 respectively). The second and third lines describe how many images were best segmented with 2 and 3 thresholds respectively. The other three lines describe how many images where best segmented with 1,2 and 3 thresholds respectively with the FF and BF methods resulting in the same thresholds amount.

From Table 2, it is possible to reaffirm the observations made from Fig. 5, that generally, 3 thresholds produce a better segmentation than 2 which, in turn, is still better than 1 threshold (binarization). This can be explained due to the matrix normalization. The brighter the $M_{i,j}$ cell, the closer the j-th threshold segmentation is to the manual segmentation. So, it is possible to conclude that this approximation gets higher as the j value increases. That is, if the goal of the threshold segmentation is to find the threshold set that results in a segmentation that is close to the manual one, then, to use 3 thresholds is more efficient than 2 which in turn is better than 1. However, one can speculate that beyond 3 thresholds, the results tend to get worse since this leads to the over-segmentation of the image. But this is a further investigation out of the current scope.

8 Conclusions

This paper presented the application of a meta-heuristic inspired by the fireflies behavior for multi-thresholding image segmentation. The proposed method's results were compared with the results of exhaustive search for 1, 2 and 3 thresholds through a manually segmented database. By searching all the solution's up to 3 thresholds space, we were able to establish a lower limit for the comparison with the manual segmentation results. This limit is useful for other algorithms or thresholds-based segmentation strategies.

The experiments indicate that the FF results are close to the exhaustive search. Moreover, these results suggest that, for threshold-based segmentation, separating the image into four groups with three thresholds, provides better chances to reach the edges obtained with the manual segmentation as a final result than dividing into three groups. Furthermore, this last separation is still closer to the manual results than the separation in two groups, the so-called binarization.

Another important point is that, as the thresholds quantity raises, the exhaustive search method's computing time tend to grow exponentially. Since the results of the FF Meta-Heuristics are very close to the brute-force method, its linear computing time is an attractive alternative to find a solution that is approximately 10 % different from the optimum result.

References

1. Pun T (1981) Entropic thresholding: a new approach. Comput Graphics Image Process 16:210–239
2. Kapur JN, Sahoo PK, Wong AKC (1985) A new method for gray-level picture thresholding using the entropy of the histogram. Comput. Graphics Image Process 29:273–285
3. Abutaleb AS (1989) A new method for gray-level picture thresholding using the entropy of the histogram. Comput Graphics Image Process 47:22–32
4. Li CH, Lee CK (1993) Minimum cross entropy thresholding. Pattern Recognit 26:617–625
5. Pal NR (1996) On minimum cross entropy thresholding. Pattern Recognit 26:575–580

6. Sahoo P, Soltani S, Wong A, Chen Y (1988) A survay of thresholding techniques. Comput Vis Gr Image Process 41(1):233–260
7. Chang C-I, Du Y, Wang J, Guo S-M, Thouin P (2006, Dec.) Survey and comparative analysis of entropy and relative entropy thresholding techniques. IEEE Proc, Vis, Image Signal Process 153(6):837–850
8. Albuquerque M, Esquef I, Mello A (2004) Image thresholding using tsallis entropy. J Stat Phys 25:1059–1065
9. Tsallis C (1999, March) Nonextensive statistics: theoretical, experimental and computational evidences and connections. Braz J Phys 29(1):1–35
10. Yin PY (2007) Multilevel minimum cross entropy threshold selection based on particle swarm optimization. Appl Math Comput 184:503–513
11. Horng MH, Liou RJ (2011) Multilevel minimum cross entropy threshold selection based on firefly algorithm. Expert Syst Appl 38:14805–14811
12. Martin D, Fowlkes C, Tal D, Malik J (2001, July) A database of human segmented natural images and its application to evaluating segmentation algorithms and measuring ecological statistics. In: Proc. 8th Int'l Conf. Computer Vision, vol 2, pp 416–423
13. Yang XS (2009) Firefly algorithms for multimodal optimization. Stochastic algorithms: fundation and applications, SAGA 2009. Lecture Notes Computer Science 5792:169–178
14. Erdmann H, Lopes LA, Wachs-Lopes G, Ribeiro MP, Rodrigues PS (2013) A study of firefly meta-heuristic for multithresholding image segmentation. In: VIpImage: Thematic Conference on Computational Vision and Medical Image Processing, Ilha da Madeira, Portugal, October, 14 to 16 2013, pp 211–217
15. Lukasik S, Zak S (2009) Firefly algorithm for continuous constrained optimization tasks. In: 1st International Conference on Computational Collective Intelligence, Semantic Web, 5-7 October 2009.
16. Dorigo M (1992) Optimization, learning, and natural algorithms. Ph. D. Thesis, Dipartimento di Elettronica e Informazione, Politecnico di Milano, Italy
17. Glover F (1989) Tabu search. PART I, ORSA J Comput 1:190–206
18. Kennedy J, Goldberg RC (1997) Particle swarm optimization. In: Proceedings of IEEE International Conference on Neural Networks, vol IV, pp 1942–1948
19. Goldberg DE (1997) Genetic algorithms in search, optimization, and machine learning. Addison Wesley, Reading
20. Hassanzadeh T, Vojodi H, Eftekhari AM (2011) An image segmentation approach based on maximum variance intra-cluster method and firefly algorithm. In: Seventh International Conference on Natural Computation, IEEE, Ed., Shanghai, China, pp 1844–1848
21. Shannon C, Weaver W (1948) The mathematical theory of communication. University of Illinois Press, Urbana
22. Tavares AHMP (2003) Aspectos matemáticos da entropia. Master Thesis, Universidade de Aveiro
23. Giraldi G, Rodrigues P (2009) Improving the non-extensive tsallis non-extensive medical image segmentation based on tsallis entropy. Pattern Analysis and Application, vol. Submitted
24. Rodrigues P, Giraldi G (2009) Computing the q-index for tsallis non-extensive image segmentation. In XXII Brazilian Symposium on Computer Graphics and Image Processing (Sibgrapi 2009), SBC, Ed., vol. To Appear
25. Sezgin M, Sankur B (2004, Jan) Survay ove image thresholding techniques and quantitative performance evaluation. J Eletr Imaging 13(1):146–165